Available online at www.sciencedirect.com

SCIENCE DIRECT®

Nanomedicine: Nanotechnology, Biology, and Medicine 2 (2006) 95–102

nanomedicine

www.nanomedjournal.com

Materials Science

Structure-based design of peptides that self-assemble into regular polyhedral nanoparticles

Senthilkumar Raman, MS, Gia Machaidze, PhD, Ariel Lustig, PhD, Ueli Aebi, PhD, Peter Burkhard, PhD*

M.E. Müller Institute for Structural Biology, Biozentrum, University of Basel, Basel, Switzerland

Received 22 February 2006; accepted 7 April 2006

Abstract Artificial particulate systems such as polymeric beads and liposomes are being applied in drug delivery, drug targeting, antigen display, vaccination, and other technologies. Here we used computer modeling to design a novel type of nanoparticles composed of peptides as building blocks. We verified the computer models via solid-phase peptide synthesis and biophysical analyses. We describe the structure-based design of a novel type of nanoparticles with regular polyhedral symmetry and a diameter of about 16 nm, which self-assembles from single polypeptide chains. Each peptide chain is composed of two coiled coil oligomerization domains with different oligomerization states joined by a short linker segment. In aqueous solution the peptides form nanoparticles of about 16 nm diameter. Such peptide nanoparticles are ideally suited for medical applications such as drug targeting and drug delivery systems, such as imaging devices, or they may be used for repetitive antigen display.

Key words: Peptide nanoparticles; Antigen display; Drug targeting; Drug delivery; Protein design

Researchers are finding a variety of biomedical applications for nanoparticles such as liposomes or polymeric beads in drug delivery, drug targeting, vaccination, protein separation, enzyme immobilization, and blood cell substitution [1-6]. Liposomes have a flexible, cell-like lipid bilayer surface that acts as a permeability barrier to trap compounds in their aqueous interior. However, liposomes can be mechanically unstable and their loading capacity limited by the water solubility of the material to be loaded.

Other approaches for the preparation of spherical polymer shells in the size range of nanometers to microns can involve, for example, the layer-by-layer deposition of polyelectrolytes on the surface of a charged nanoparticle and subsequent dissolution of the templating particle, or the self-assembly of amphiphilic diblock or triblock copolymers into micelles, selective cross-linking of their hydrophilic shell, and subsequent degradation of the hydrophobic core [7]. Preparation of such nanocapsules is complex and may be ineffective. Also, polymeric beads, though mechanically more stable with a larger loading capacity than liposomes, lack many of the useful surface properties of a lipid bilayer shell. Furthermore, they do not biodegrade easily and hence may be toxic.

Here we present the structure-based design of mechanically and chemically stable nanoparticles, using the ability of peptides and proteins to self-assemble into particles of well-defined size and shape. Once assembled these peptide nanoparticles can serve as vehicles for drug targeting. Currently used drug targeting systems include, for example, antibodies that deliver radioactive isotopes to proliferating blood vessels [8] and peptides that target tumor blood vessels [9].

Alternatively, peptide nanoparticles can be used as repetitive antigen display systems for the development of vaccines. During the past decade several immunogenic vaccination strategies have been identified [10-14]. However, at this point vaccines for many pathogens worldwide, including malaria (*Plasmodium falciparum*) [15], *Mycobacterium tuberculosis* [16], group A streptococci [17], hepatitis viruses [11], herpesviruses [18], human immunodeficiency virus (HIV) [10,12], and influenza [19], are still ineffective or simply unavailable.

No financial conflict of interest was reported by the authors of this paper.

This research was supported by the M.E. Müller Foundation and the NCCR Nanoscale Science (SNF). The authors would like to thank J. Engel and W. Meier for critical reading of the manuscript.

* Corresponding author. The Institute of Materials Science, University of Connecticut, Storrs, CT 06269-3136, United States.

E-mail address: peter.burkhard@uconn.edu (P. Burkhard).

1549-9634/$ – see front matter © 2006 Elsevier Inc. All rights reserved.
doi:10.1016/j.nano.2006.04.007

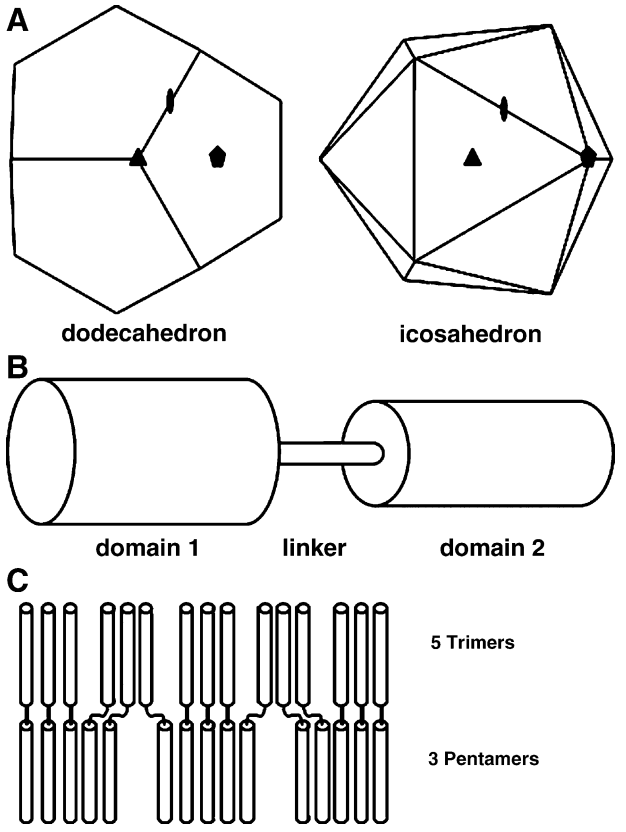

Fig 1. Basic concepts of the design. **A,** Possible regular polyhedra built from two-, three-, and five-fold symmetry elements. The symmetry elements are denoted as black symbols. The dodecahedron and the icosahedron have the same internal symmetry elements and are built from 60 identical 3-dimensional building blocks (asymmetric units). **B,** Architecture of the monomeric building block for self-assembly into regular polyhedra. The building block is composed of an oligomerization domain 1, a linker domain, and a second oligomerization domain. **C,** Even units consisting of trimers and pentamers. The number of monomers (building blocks) is defined by the least common multiple (LCM) of the oligomerization states of the two domains 1 and 2 of the building blocks.

Because of the broad range of humoral and cellular immune responses they elicit as well as the memory responses they induce, live attenuated vaccines are still the vaccines of choice [10-14]. From a practical point of view, however, live attenuated vaccines raise issues related to manufacturing and safety that may preclude their widespread use [10-14]. As an alternative, peptide-based vaccines have been developed and used for vaccination. However, synthetic peptides alone are often not immunogenic enough, and a strong immunoadjuvant is usually included to enhance their immunogenicity. There remain concerns, however, about toxic adjuvants, which are critical to the immunogenicity of synthetic peptides [20-22].

Because their architecture is similar to that of virus capsids, the peptide nanoparticles described here combine the strong immunogenic effect of live attenuated vaccines with the purity and high specificity in eliciting immune responses of peptide-based vaccines, while avoiding both the safety risks of live attenuated vaccines and the need for toxic adjuvants of peptide-based vaccines.

Table 1
Possible combinations of oligomerization states

ID	Domain 1	Domain 2	Polyhedron type	LCM	No. of even units	No of asymmetric units
1	5	2	Dodecahedron/ icosahedron	10	6	60
2	5	3	Dodecahedron/ icosahedron	15	4	60
3	4	3	Cube/ octahedron	12	2	24
4	3	4	Cube/ octahedron	12	2	24
5	3	5	Dodecahedron/ icosahedron	15	4	60
6	2	5	Dodecahedron/ icosahedron	10	6	60
7a*	5	4	Irregular	20	1	20
7b*	4	5	Irregular	20	1	20

* The entries 7a and 7b do not correspond to regular polyhedra but represent the largest even units that may be formed with oligomerization states ranging from 2 to 5.

Methods

Peptide synthesis

The peptide was synthesized by Peptide Specialities (Heidelberg, Germany). Its purity (>95%) was verified by high-performance liquid chromatography and mass spectrometric analyses.

Refolding of the peptide

The peptide folding procedure was carried out under four different regimes.

Preparation 1 (oxidizing conditions)

1 mg/mL peptide was dissolved directly in 150 mM NaCl, 20 mM Tris pH 7.5.

Preparation 2 (reducing conditions)

1 mg/mL peptide was dissolved directly in 150 mM NaCl, 20 mM Tris pH 7.5, 2 mM dithiothreitol (DTT).

Preparation 3 (denaturation, renaturation under oxidizing conditions)

0.07 mg/mL peptide was dissolved in 150 mM NaCl, 20 mM Tris pH 7.5, 2 mM DTT, 8 M urea. The solution was then dialyzed in steps from 150 mM NaCl, 20 mM Tris, pH 7.5; 8 M urea/4 M urea/2 M urea/no urea. Finally, the solution was concentrated to 1 mg/mL in 150 mM NaCl, 20 mM Tris pH 7.5.

Preparation 4 (denaturation, renaturation under reducing conditions)

0.07 mg/mL peptide was dissolved in 150 mM NaCl, 20 mM Tris pH 7.5, 8 M urea, 2 mM DTT. The solution was then dialyzed in steps from 150 mM NaCl, 20 mM Tris pH 7.5, 8 M urea and 2 mM DTT/4 M urea and 2 mM DTT/ 2 M urea and 2 mM DTT/no urea and 2 mM DTT/no urea

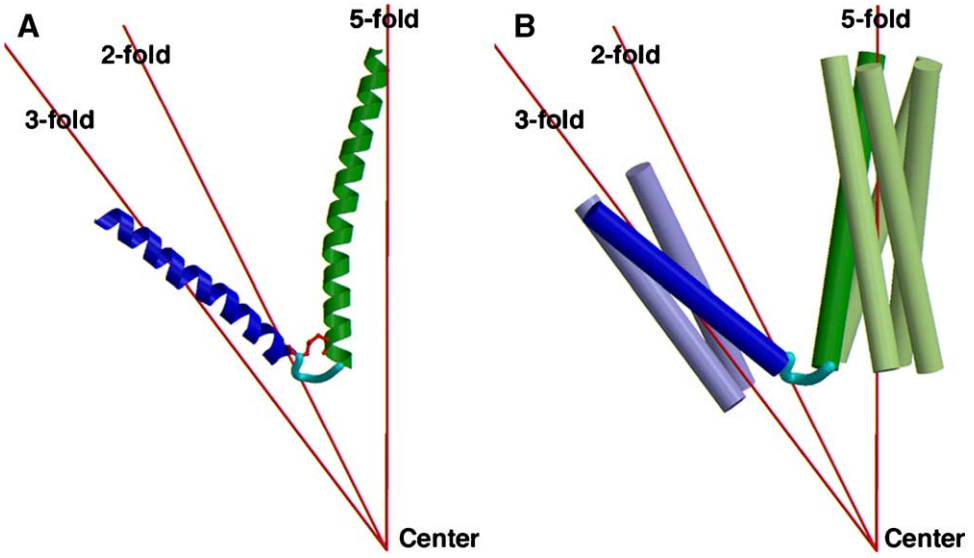

Fig 2. Internal symmetry elements of the dodecahedron. **A,** A 3D building block composed of domain 1 (blue; coiled coil domain with three-fold symmetry), a linker segment (cyan), and domain 2 (green; coiled coil domain with five-fold symmetry) is displayed such that the internal symmetry elements of the domains 1 and 2 are superimposed onto the symmetry axes of the polyhedron. The intrahelical disulfide bridge between the helices is displayed in red. **B,** The complete coiled coil domains are displayed as cylinders. The additional symmetry objects generated by the three-fold and the five-fold rotational symmetry elements of the polyhedron are displayed in light colors, whereas the original molecule is displayed in dark colors. The rotational symmetry axes (two-fold, three-fold, and five-fold) are displayed as red lines in **A** and **B**.

and no DTT. Finally the solution was concentrated to 1 mg/mL in 150 mM NaCl, 20 mM Tris pH 7.5.

Analytical ultracentrifugation

Analytical ultracentrifugation (AUC) was carried out on an Optima XL-A analytical ultracentrifuge (Beckman Instruments, Palo Alto, CA) equipped with a 12-mm Epon double-sector cell in an An-60 Ti rotor. Sedimentation equilibrium runs were performed at 20°C at rotor speeds between 5200 and 15,000 rpm and peptide concentrations of 0.15 to 1.0 mg/mL. Average molecular masses were evaluated by using a floating baseline computer program that adjusts the baseline absorbance to obtain the best linear fit of ln(absorbance) versus the square of the radial distance. A partial specific volume of 0.73 mL/g was used.

Electron microscopy

Specimens were prepared for electron microscopy (EM) by negative staining with 2% uranyl acetate and at a peptide concentration of 0.01 mg/mL. They were analyzed and photographed on a Zeiss EM910 transmission electron microscope (Carl Zeiss, Oberkochen, Germany).

Results

Design principles

There exist only five regular polyhedra: the tetrahedron, the cube, the octahedron, the dodecahedron, and the icosahedron. These polyhedra show different internal rotational symmetry elements; for example the dodecahedron and the icosahedron have two-fold, three-fold, and five-fold rotational symmetry axes (Figure 1, *A*). The cube and the octahedron are built up from 24 asymmetric units, whereas the dodecahedron and icosahedron are built up from 60 asymmetric units, thus generating the largest closed shell in which every subunit is in an identical environment [23] (Table 1). These asymmetric units are tri-pyramids, and each of the pyramid edges corresponds to one of the rotational symmetry axes; hence the edges of these asymmetric units represent two-fold, three-fold, four-fold, or five-fold symmetry axes depending on the type of polyhedron. If the symmetry axes of peptidic oligomerization domains are superpositioned onto the edges of these tri-pyramids, such 3-dimensional building blocks can be built up from peptidic oligomerization domains (Figure 2, *A* and *B*). As a consequence, it may be possible to design a peptide nanoparticle with regular polyhedral symmetry by connecting peptidic oligomerization domains with different oligomerization states. Hence, to construct a nanoparticle as a regular dodecahedron, a continuous peptide chain comprising a trimerization domain, a short linker sequence, and a pentamerization domain is needed (Figures 1, *B* and 2, *A*). Such a continuous peptide chain will be the basic building block of the nanoparticle, the content of one asymmetric unit. A similar approach using dimeric and trimeric proteins joined in a specific angle by means of a rigid α-helical linker between the two building blocks has been presented by Padilla et al. [24].

Protein oligomerization domains are well known; the most simple and most abundant oligomerization domain is probably the coiled coil folding motif [25,26]. This oligomerization motif has been shown to exist as a dimer, trimer, tetramer, and pentamer. Some of the best-known

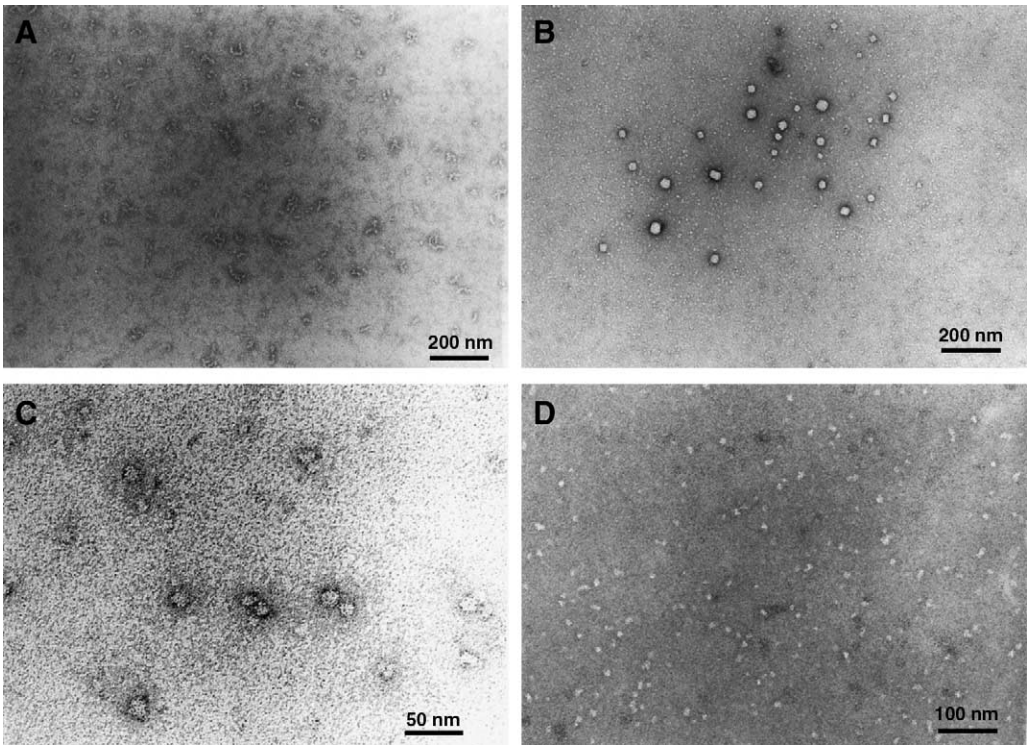

Fig 3. Electron micrographs of the peptide nanoparticles. **A,** The peptide nanoparticles formed under oxidizing conditions (preparation 1). **B,** The peptide nanoparticles formed under reducing conditions (preparation 2). **C,** The peptide nanoparticles formed under oxidizing conditions after denaturation (preparation 3). **D,** The peptide nanoparticles formed under reducing conditions after denaturation (preparation 4). The pictures were prepared by negative staining with 2% uranyl acetate; the concentration of the peptide was 0.01 mg/mL. In **B** the average diameter of the particles is roughly 25 nm. In **C** and **D** the average diameter of the particles is roughly 16 nm.

examples are the GCN4 leucine zipper [27], fibritin [28], tetrabrachion [29], and cartilage oligomerization matrix protein (COMP) [30], representing dimeric, trimeric, tetrameric, and pentameric coiled coils, respectively. Other simple oligomerization motifs are also known, such as the trimerization domain (the so-called foldon) of fibritin [28].

If these monomeric building blocks consisting of a continuous peptide chain composed of two linked oligomerization domains with different oligomerization states assemble, they will first form "even units" (Figure 1, *C*). The number of monomers that will assemble into such an even unit is defined by the least common multiple (LCM) of their oligomerization states. Hence if the oligomerization domains of the monomeric building block consist of a trimer and a pentamer, 15 monomers will form an even unit. The geometry of these even units, however, may not be regular. Several of these even units may then further assemble into larger nanoparticles (cf. Table 1). For example, to form a dodecahedron four even units composed of 15 monomeric building blocks each are needed; that is, the nanoparticle with regular geometry will be composed of 60 monomeric building blocks (see Figure 4, *A*). The possible combinations of oligomerization states of the two domains to form any of the regular polyhedra are shown in Table 1.

Whether the even units will assemble additionally to form a regular polyhedron depends on (1) the interactions at the interface between neighboring oligomerization domains within a nanoparticle, (2) the length of the linker segment, and (3) the shape of the individual oligomerization domains. Optimizing the interactions at the interface between neighboring domains can significantly improve the packing and stability of the regular polyhedron. Such improvements can be achieved by optimizing the hydrophobic and the ionic interactions between the interacting oligomerization domains or by their chemical cross-linking, for example by introducing cysteine residues so that a disulfide bridge is formed between two interacting oligomerization domains (cf. Figure 2, *A*). The linker domain should be long enough to avoid disruption of the protein fold of the oligomerization domains but short enough to maintain close contact between the two oligomerization domains.

Self-assembly of nanoparticles

According to the principles outlined above [31] we have rationally designed a peptide nanoparticle composed of a monomeric building block with the following sequence:

```
1         10        20        30        40        50        60
Ac-DEMLRELQETNAALQDVRELLRQQVKQITFLKCLLMGGRLLCRLEELERRLEELERRLEELERR-NH2
```

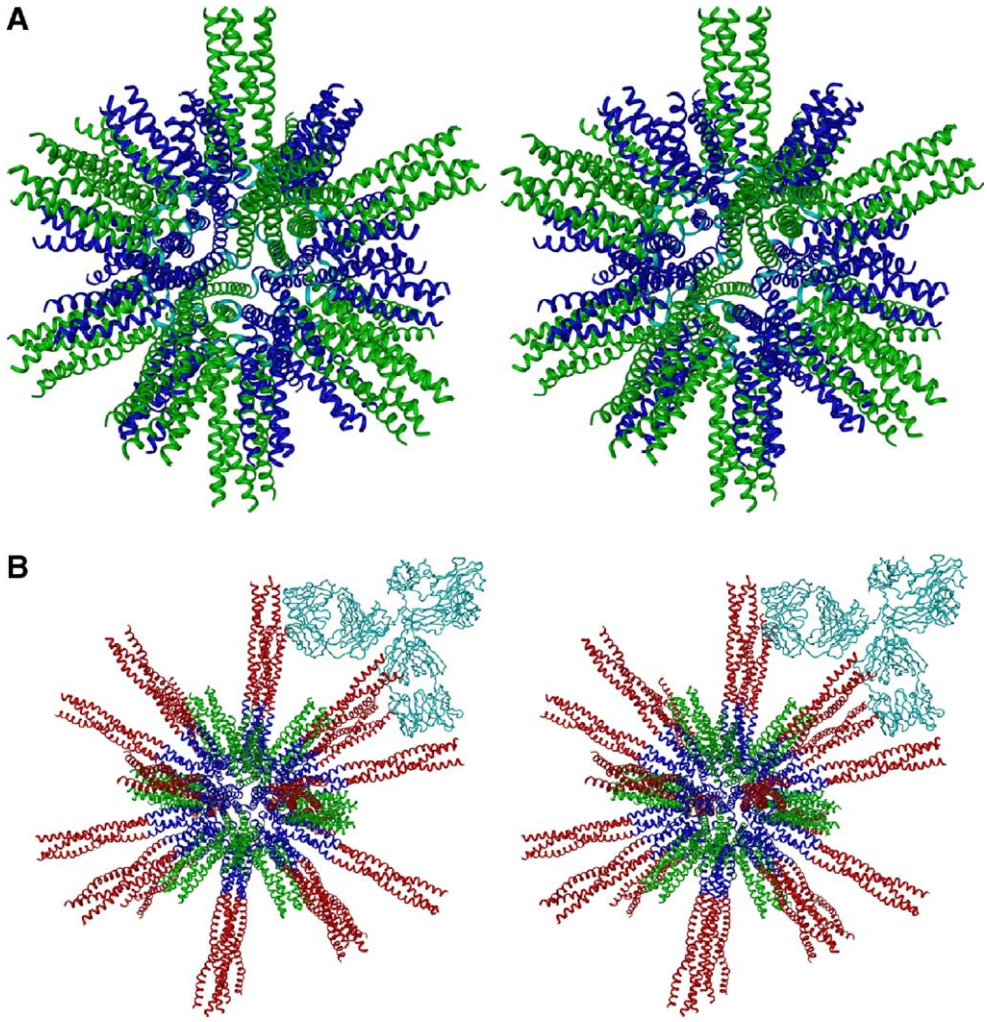

Fig 4. Stereo picture of a computer model of the complete peptide nanoparticle with dodecahedral symmetry. **A,** The particles are composed from the pentameric coiled coil domain of COMP (green) and a trimeric de novo designed coiled coil domain (blue). The calculated diameter of this particle is about 16 nm. **B,** The same nanoparticle as in **A** but wherein the trimeric coiled coils are further extended by the coiled coil sequence of the HIV surface protein gp41 (red). This portion of the gp41 protein is ideally displayed in many copies on the surface of the nanoparticle to be recognized by an antibody (cyan), thus eliciting a strong immune response.

The 36 N-terminal amino acids (green) of this peptide correspond to the slightly modified pentameric coiled coil domain of COMP [30]. The 26 C-terminal amino acids (blue) correspond to a de novo-designed minimal trimeric coiled coil domain according to the principles as outlined by Burkhard et al. [32-34]. These two oligomerization domains with different oligomerization states are joined by a linker segment consisting of two glycine residues (black). According to model building three of the four C-terminal residues of COMP have been modified to optimize interhelical contacts between the two oligomerization domains including an intramolecular disulfide bridge. The cysteine residues in position 33 and 42 are optimally placed for such an intramolecular disulfide bridge between the helices. They are at **f** positions in the heptad repeats of the respective coiled coils and one turn away from the respective helix ends (cf. Figure 2, *A*) and may form a disulfide bridge without disturbing the coiled coil geometry of the two oligomerization domains. Finally, the positively charged N-terminal amino group is replaced by an acetyl moiety and the negatively charged C-terminal carboxyl group is replaced by an amide group to avoid destabilization of the helices due to their helix-macrodipole [33].

Because of the complexities of folding of a protein containing intramolecular disulfide bridges, four different refolding conditions were tested for their assembly into polyhedral nanoparticles (for details see Methods). In a first regime (preparation 1) the assembly process of the peptide at a relatively high concentration was performed under oxidizing conditions, allowing for disulfide bridge formation. To test whether the intramolecular disulfide bridge is needed for proper self-assembly of the peptide into particles with regular dodecahedral symmetry, the peptide, again at relatively high concentration, was assembled under reducing conditions (preparation 2).

Because high peptide concentrations can lead to intermolecular disulfide bridge formation and consequently to aggregation, we tested two other refolding regimes. The peptide concentration was reduced to minimize intermolecular contacts, and then the peptide was completely denatured in 8 M urea. Then the refolding process was started by a stepwise dialysis of the urea under either oxidizing (preparation 3) or reducing (preparation 4) conditions. In a final step of preparation 4 the disulfide bridges were allowed to form by changing to oxidizing conditions.

The assembly behavior of the nanoparticles under these four regimes was analyzed by AUC to determine the molecular weight of the aggregates. Furthermore, the morphology of the aggregates was investigated by EM.

In preparation 1 (1 mg/mL) AUC revealed a mixture of components with molecular weights ranging from about 380 to 2200 kDa corresponding to aggregates of 48 to 280 monomers. Accordingly, electron micrographs showed that the peptides do not form spherical nanoparticles but instead form elongated irregular aggregates (Figure 3, *A*).

AUC of preparation 2 (1 mg/mL) revealed again a mixture of components with molecular masses ranging from about 130 to 330 kDa. This corresponds to nanoparticles composed of about 16 to 42 monomers. The lowest molecular mass components roughly correspond to even units (cf. Figure 1, *C*), which are composed of 15 peptide chains. In contrast to preparation 1, under reducing conditions the peptides do form nanoparticles as shown by EM (Figure 3, *B*). The size of these nanoparticles is variable, however, with diameters ranging from about 15 to 45 nm, but they are not always completely spherical.

The refolding processes starting at lower peptide concentrations and complete denaturation of the peptide gave much more homogeneous results. The measured molecular mass of the particles from preparation 3 was only slightly concentration dependent (Table 2). At lower final peptide concentrations the nanoparticles are composed of three even units, whereas at higher final peptide concentrations they are composed of four even units. The latter is in agreement with nanoparticles with regular dodecahedral symmetry being composed of four even units or 60 monomeric peptide chains, respectively (Table 1). As judged by EM the peptide forms nanoparticles of roughly homogeneous size and spherical appearance (Figure 3, *C*). The diameter of these nanoparticles is about 16 nm, in good agreement with the value predicted for a modeled regular dodecahedron.

By AUC the measured molecular mass of the particles from preparation 4 is again concentration dependent (Table 2). Their sizes range from particles composed of 80 to as many as about 121 peptide chains. Again, the peptides form nanoparticles of nearly identical size with mostly spherical appearance (Figure 3, *D*). The diameter of the peptide nanoparticles is very similar to that of the particles from preparation 3. These micrographs were taken for samples assembled at low peptide concentrations, conditions under which their molecular mass was shown to be close to that of particles with regular dodecahedral symmetry (Table 2).

Table 2
Molecular masses of nanoparticles

	Concentration (mg/mL)	MW (kDa)	No. of monomers	No. of even units
Preparation 3	0.15	347	43.9	2.9
	0.3	356	45.1	3.0
	0.4	461	58.4	3.9
	0.6	437	55.3	3.7
	0.8	489	61.9	4.1
Preparation 4	0.15	633	80.1	5.3
	0.25	718	90.9	6.1
	0.8	960	121.5	8.1

Discussion

The peptide sequence outlined above was rationally designed so as to form nanoparticles showing regular polyhedral symmetry, that is, consisting of 60 monomeric building blocks (see Figure 4, *A*). Computer modeling predicted that such a particle would have a diameter of about 16 nm and a molecular mass of 473 kDa, corresponding to a particle composed of 60 monomeric peptide chains (see Table 2). The appropriate folding regime was crucial to obtain a homogeneous population of nanoparticles with regular polyhedral symmetry. This can be rationalized by the different possibilities of disulfide formation during the refolding process. In high peptide concentrations the peptide chains may easily form intermolecular disulfide bridges leading to irregular aggregates (cf. Figure 3, *A*). Such a behavior was observed in the refolding procedure of preparation 1: EM revealed elongated aggregates devoid of any regular structure. The oligomerization properties of the peptide made of two distinct oligomerization domains joined by a linker segment, when combined with the formation of intermolecular disulfide bridges between different peptide chains, leads to a network of peptides, which are cross-linked either by oligomerization of the coiled coil domains or by intermolecular disulfide bridges.

Therefore, it is crucial to avoid intermolecular disulfide bridge formation during refolding. Keeping the system under reducing conditions in the refolding process (preparation 2) leads to the formation of spherical nanoparticles. However, by EM the nanoparticles are not of unique appearance, either in shape or in size (Figure 3, *B*). This result is in agreement with those obtained by AUC, showing that under these conditions the peptide can form particles of different sizes. The measured molecular mass represents a distribution of particles of various sizes. The smaller particles in Figure 3, *B* presumably correspond to even units composed of 15 monomers (roughly corresponding to the smallest measured molecular mass; cf. Table 2), whereas the larger particles are multiples thereof. When the intramolecular disulfide bridge is missing, the peptide does form spherical nanoparticles but not with regular dodecahedral symmetry. This documents the

importance of the intramolecular disulfide bridge for proper formation of nanoparticles with regular symmetry.

The aim was to avoid intermolecular disulfide bridge formation while allowing for intramolecular disulfide bridge formation. The coiled coil domains of COMP and of the de novo-designed trimer are known to form very stable oligomers [34,35]. During refolding out of 8 M urea these coiled coil domains will already form in urea concentrations that are moderately high. Formation of the helices within the two coiled coil domains will bring the two cysteines of the same peptide chain into close contact (cf. Figure 2, *A*). Furthermore, they will be located close to the center of the even units and/or the regular dodecahedral particles; hence they are shielded from the solvent and no longer accessible for intermolecular contacts. Under oxidizing conditions (preparation 3) intramolecular disulfide bridge formation will then immediately and predominantly occur while avoiding intermolecular cross-linking. However, also under reducing conditions (preparation 4) the cysteine residues cannot form intermolecular disulfide bridges and the intramolecular disulfide bridge will be formed only when changing to oxidizing conditions in a final step, that is, when the cysteine residues are already shielded from the solvent.

The intramolecular disulfide bridge between the two helices of adjacent oligomers fixes the spatial orientation of the two helices relative to each other. In agreement with our design, this disulfide bridge proves to be a prerequisite for the effective formation of nanoparticles with regular dodecahedral symmetry.

Conclusions

Such nanoparticles with regular polyhedral symmetry represent an ideal repetitive antigen display system. Surface proteins of pathogens or fragments of such proteins can easily be engineered into the peptide sequence of the nanoparticle. Notably, many surface proteins of pathogens contain coiled coil sequences. For example, by simply extending the trimeric coiled coil of the nanoparticle by the coiled coil sequence of the HIV surface protein gp41, a HIV vaccine candidates can be designed (Figure 4, *B*). The predicted strong immune response against such a vaccine can be rationalized by the optimal binding geometry of an IgG molecule to the nanoparticle (cf. Figure 4, *B*). Whereas in the past, different kinds of adjuvants were tested to improve the immunogenicity of an antigen or a specific epitope, such a repetitive antigen display can strongly augment the immunogenicity of a certain epitope [36], thus avoiding the need for sometimes highly toxic adjuvants [37]. We have designed peptide nanoparticles aimed at eliciting a strong immune response, and our preliminary immunization results confirm the correctness of this hypothesis.

References

[1] Langer R. Drug delivery and targeting. Nature 1998;392:5-10.

[2] Kiser PF, Wilson G, Needham D. A synthetic mimic of the secretory granule for drug delivery. Nature 1998;394:459-62.

[3] Ong S, Liu H, Qiu X, Bhat G, Pidgeon C. Membrane partition coefficients chromatographically measured using immobilized artificial membrane surfaces. Anal Chem 1995;67:755-62.

[4] Rogers JA, Choi YW. The liposome partitioning system for correlating biological activities of imidazolidine derivatives. Pharm Res 1993;10:913-7.

[5] Savic R, Luo L, Eisenberg A, Maysinger D. Micellar nanocontainers distribute to defined cytoplasmic organelles. Science 2003;300:615-8.

[6] Allen TM, Cullis PR. Drug delivery systems: entering the mainstream. Science 2004;303:1818-22.

[7] Meier W. Polymer nanocapsules. Chem Soc Rev 2000;29:295-303.

[8] Tabata M, Kondo M, Haruta Y, Seon BK. Antiangiogenic radioimmunotherapy of human solid tumors in SCID mice using 125I-labeled anti-endoglin monoclonal antibodies. Int J Cancer 1999;82:737-42.

[9] Arap W, Pasqualini R, Ruoslahti E. Cancer treatment by targeted drug delivery to tumor vasculature in a mouse model. Science 1998;279:377-80.

[10] Berzofsky JA, Ahlers JD, Derby MA, Pendleton CD, Arichi T, Belyakov IM. Approaches to improve engineered vaccines for human immunodeficiency virus and other viruses that cause chronic infections. Immunol Rev 1999;170:151-72.

[11] Lechmann M, Liang TJ. Vaccine development for hepatitis C. Semin Liver Dis 2000;20:211-26.

[12] Paul WE. Can the immune response control HIV infection? Cell 1995;82:177-82.

[13] Gahery-Segard H, Pialoux G, Charmeteau B, Sermet S, Poncelet H, et al. Multiepitopic B- and T-cell responses induced in humans by a human immunodeficiency virus type 1 lipopeptide vaccine. J Virol 2000;74:1694-703.

[14] Gras-Masse H. Single-chain lipopeptide vaccines for the induction of virus-specific cytotoxic T cell responses in randomly selected populations. Mol Immunol 2001;38:423-31.

[15] Hoffman SL, Subramanian GM, Collins FH, Venter JC. *Plasmodium*, human and *Anopheles* genomics and malaria. Nature 2002;415:702-9.

[16] Wang J, Zganiacz A, Xing Z. Enhanced immunogenicity of BCG vaccine by using a viral-based GM-CSF transgene adjuvant formulation. Vaccine 2002;20:2887-98.

[17] Hayman WA, Toth I, Flinn N, Scanlon M, Good MF. Enhancing the immunogenicity and modulating the fine epitope recognition of antisera to a helical group A streptococcal peptide vaccine candidate from the M protein using lipid-core peptide technology. Immunol Cell Biol 2002;80:178-87.

[18] Nesburn AB, Burke RL, Ghiasi H, Slanina SM, Wechsler SL. Therapeutic periocular vaccination with a subunit vaccine induces higher levels of herpes simplex virus-specific tear secretory immunoglobulin A than systemic vaccination and provides protection against recurrent spontaneous ocular shedding of virus in latently infected rabbits. Virology 1998;252:200-9.

[19] Wareing MD, Tannock GA. Influenza update: vaccine development and clinical trials. Curr Opin Pulm Med 2002;8:209-13.

[20] Parmiani G, Castelli C, Dalerba P, Mortarini R, Rivoltini L, et al. Cancer immunotherapy with peptide-based vaccines: what have we achieved? Where are we going? J Natl Cancer Inst 2002;94:805-18.

[21] Van Regenmortel MH. Antigenicity and immunogenicity of synthetic peptides. Biologicals 2001;29:209-13.

[22] BenMohamed L, Wechsler SL, Nesburn AB. Lipopeptide vaccines—yesterday, today, and tomorrow. Lancet Infect Dis 2002;2:425-31.

[23] Johnson JE, Reddy VS. Biggest virus molecular structure yet! Nat Struct Biol 1998;5:849-54.

[24] Padilla JE, Colovos C, Yeates TO. Nanohedra: using symmetry to design self assembling protein cages, layers, crystals, and filaments. Proc Natl Acad Sci USA 2001;98:2217-21.

[25] Burkhard P, Strelkov SV, Stetefeld J. Coiled coils: a highly versatile protein folding motif. Trends Cell Biol 2001;11:82-8.

[26] Lupas A. Coiled coils: new structures and new functions. Trends Biochem Sci 1996;21:375-82.
[27] O'Shea EK, Klemm JD, Kim PS, Alber T. X-ray structure of the GCN4 leucine zipper, a two-stranded, parallel coiled coil. Science 1991;254:539-44.
[28] Tao Y, Strelkov SV, Mesyanzhinov VV, Rossmann MG. Structure of bacteriophage T4 fibritin: a segmented coiled coil and the role of the C-terminal domain. Structure 1997;5:789-98.
[29] Stetefeld J, Jenny M, Schulthess T, Landwehr R, Engel J, Kammerer RA. Crystal structure of a naturally occurring parallel right-handed coiled coil tetramer. Nat Struct Biol 2000;7:772-6.
[30] Malashkevich VN, Kammerer RA, Efimov VP, Schulthess T, Engel J. The crystal structure of a five-stranded coiled coil in COMP: a prototype ion channel? [see comments] Science 1996; 274:761-5.
[31] Sanner MF, Stolz M, Burkhard P, Kong XP, Min G, et al. Visualizing nature at work from the nano to the macro scale. Nanobiotechnology 2005;1:7-22.
[32] Burkhard P, Meier M, Lustig A. Design of a minimal protein oligomerization domain by a structural approach. Protein Sci 2000;9: 2294-301.
[33] Burkhard P, Kammerer RA, Steinmetz MO, Bourenkov GP, Aebi U. The coiled-coil trigger site of the rod domain of cortexillin I unveils a distinct network of interhelical and intrahelical salt bridges. Structure Fold Des 2000;8:223-30.
[34] Burkhard P, Ivaninskii S, Lustig A. Improving coiled-coil stability by optimizing ionic interactions. J Mol Biol 2002;318:901-10.
[35] Guo Y, Kammerer RA, Engel J. The unusually stable coiled-coil domain of COMP exhibits cold and heat denaturation in 4-6 M guanidinium chloride [in process citation]. Biophys Chem 2000;85:179-86.
[36] Fehr T, Skrastina D, Pumpens P, Zinkernagel RM. T cell-independent type I antibody response against B cell epitopes expressed repetitively on recombinant virus particles. Proc Natl Acad Sci USA 1998;95: 9477-81.
[37] Hunter RL. Overview of vaccine adjuvants: present and future. Vaccine 2002;20(Suppl 3):S7-12.